

Supplementary Information

Fast benchtop visualization of graphene grain boundaries using adhesion property of defects

Seong Uk Yu,^a Yeonchoo Cho,^a Beomjin Park,^b Namdong Kim,^a Il Seung Youn,^a Minhyeok Son,^a Jin Kon Kim,^b Hee Cheul Choi,^a Kwang S. Kim^{a,*}

^aDepartment of Chemistry and ^bDepartment of Chemical Engineering, Pohang University of Science and Technology, Pohang 790-784, Korea

Preparation of samples

Synthesis of graphene using CVD process: The synthesis was performed using an one inch tube-type furnace CVD system equipped with a quartz tube to protect samples from direct contact to heating coils. Cu foil (0.025 mm thick, 99.8 % purity, Alfa Aesar) was placed at the center of the furnace. The reaction was carried out for 30 min at 1000 °C while introducing 30 sccm of CH₄ and 20 sccm of H₂ at a total pressure of ~5 torr. After reaction was completed, the sample was cooled down to room temperature by opening the cover of furnace under 20 sccm of H₂ at a total pressure of ~2 torr.

Transfer of SLG grown on Cu foil to SiO₂/Si substrate: The SLG grown on a Cu foil was spin-coated with poly(methyl methacrylate) (PMMA, 495 PMMA A4, MicroChem). After hardening at 100 °C for 1 min, the PMMA/graphene/Cu foil was floated in a 1 M ferric chloride hexahydrate (FeCl₃•6H₂O, Sigma Aldrich, 97 %) solution to etch out Cu. The resulting PMMA-supported graphene was scooped out from the etchant and rinsed with deionized water several times. Then, the graphene side was placed on a target SiO₂/Si substrate and dried at 90 °C to provide better adhesion between graphene and the substrates. Finally, PMMA was removed by acetone. The transferred graphene was annealed at 300 °C

Basic permanganate treatment: Graphene on copper (Graphene/Cu) was soaked in thin layer chromatography (TLC) staining solution (basic permanganate condition), and was rinsed with distilled water. For visualization, the sample was heated by heat gun at 400 °C.

Acidic permanganate treatment: KMnO₄ (0.9g) was dissolved in 7mL H₂SO₄ at ice temperature. Graphene on copper was soaked in acidic permanganate, and was rinsed with distilled water.

Calculation Methods

The PBE functional is used with the Tkatchenko-Scheffler dispersion correction implemented in FHI-AIMS. The tier 2 basis on light atomic grids is employed for relaxation, whereas tight atomic grids are employed for single point calculations. The Tkatchenko-Scheffler scheme determines atomic dispersion coefficients based on Hirshfeld partitioning, allowing accurate prediction for any type of molecular assemblies, in contrast to other dispersion schemes which fix the coefficients.

Characterization

SEM, TEM images: Scanning electron microscopy (SEM, Hitachi, S4800) was operated at 10 kV. Transmission electron microscopy (TEM) analyses were made with a JEM-2200 electron microscope with an accelerating voltage of 120 kV. Raman spectra were carried out using a Senterra Raman Scope system with a 532 nm wavelength incident laser light and power 20 mW. Thermo Scientific K-Alpha X-ray photoelectron spectroscopy (XPS) analyses were performed with an ESCALAB-220I-XL (THERMO-ELECTRON, VG Company) device.

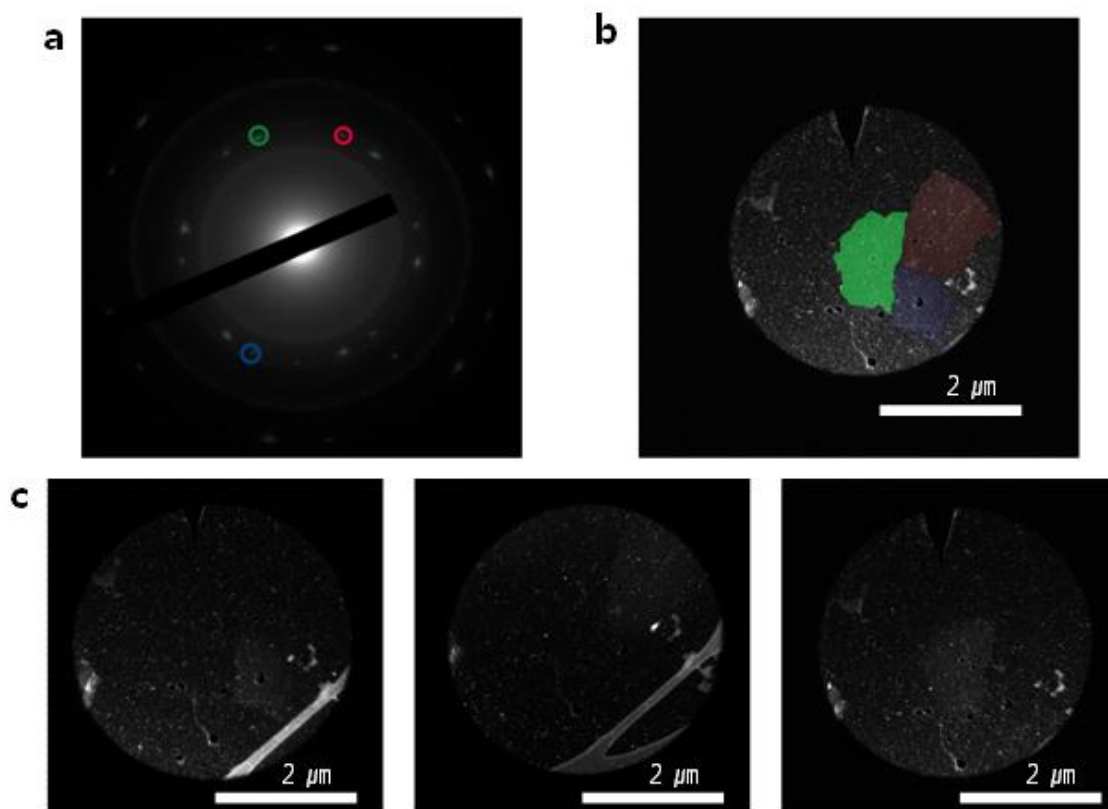


Figure 1S. Dark field TEM image of graphene¹. By placing smallest OL aperture at 3 different circular regions of diffraction patterns as marked in (a) and changing TEM mode to image-mode, each grain of graphene is distinguished as in (c). The dimension of each grain is an order of micrometers. The grain sizes in TEM image are slightly smaller than those in

SEM image because the intensity of light from marked area is too weak to make clear visualization of edges.

AFM Phase Images: (Figure 2S)

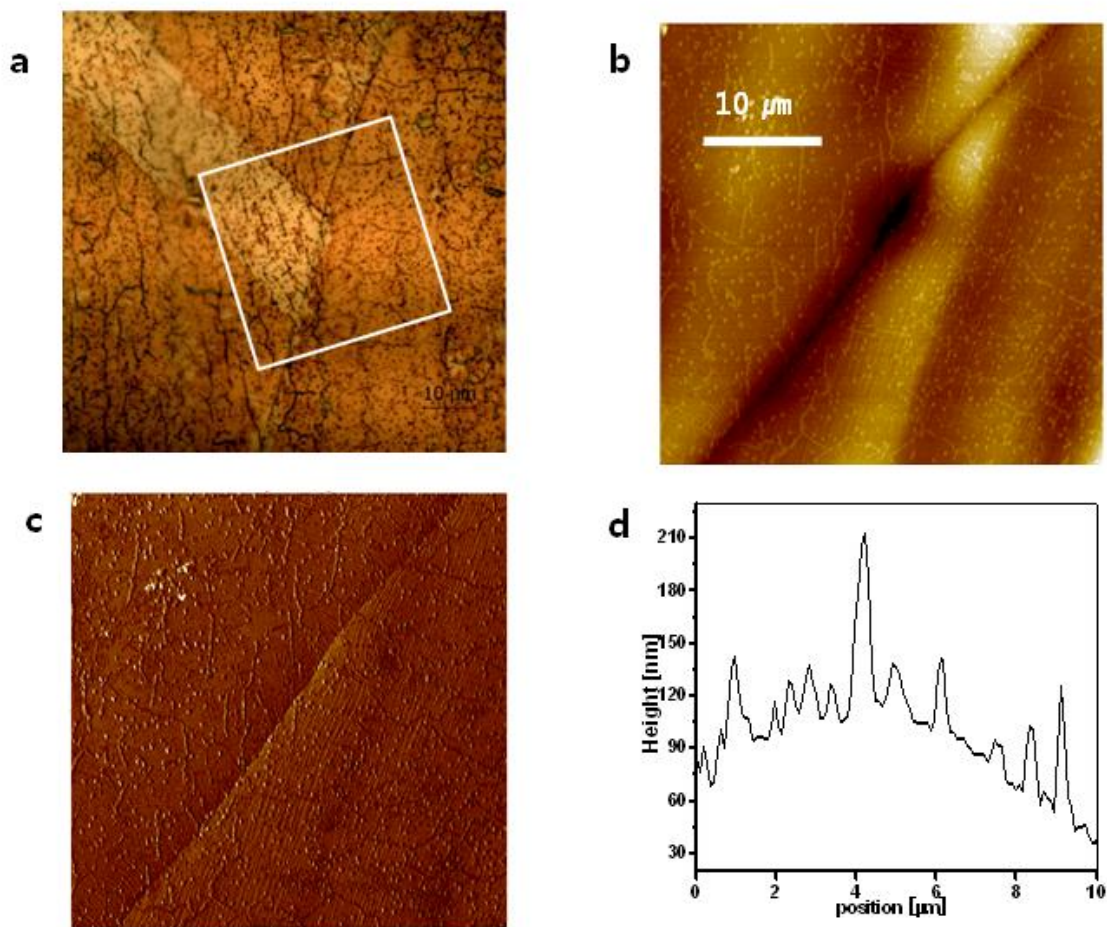


Figure 2S. Optical microscope image (a) after basic permanganate treatment and the AFM topography image (b) and phase image (c) within the rectangular box in (a). Line profile (d) on the scale bar in (b). The volume of copper increased by oxidation, and the height increased by 20~100 nm.

Raman spectra: As oxidation power increased, the G band of graphene shows the blue shift from 1587.8 cm^{-1} to 1593.96 cm^{-1} (basic) and 1596 cm^{-1} (acidic). The 2D band also shows blue-shifted. These blue shifts indicate the oxidation of graphene². As oxidation power increases, the D band is intensified.

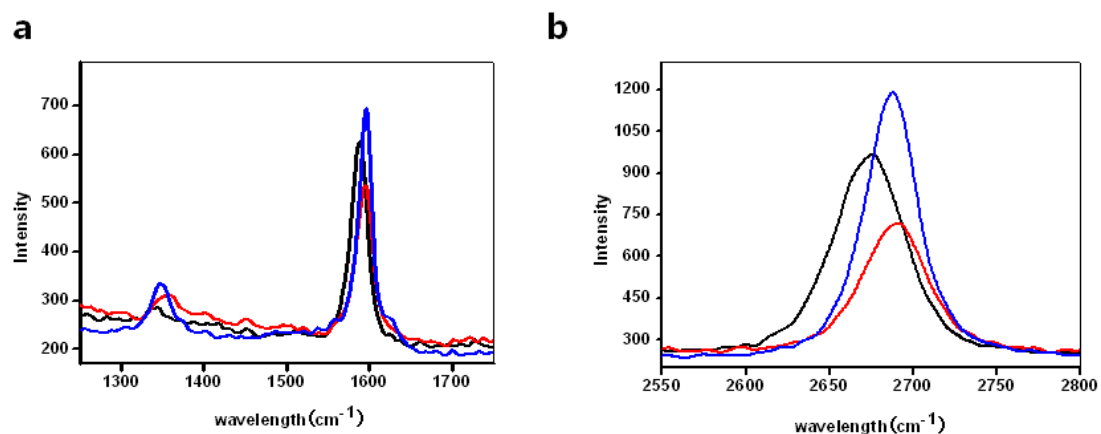
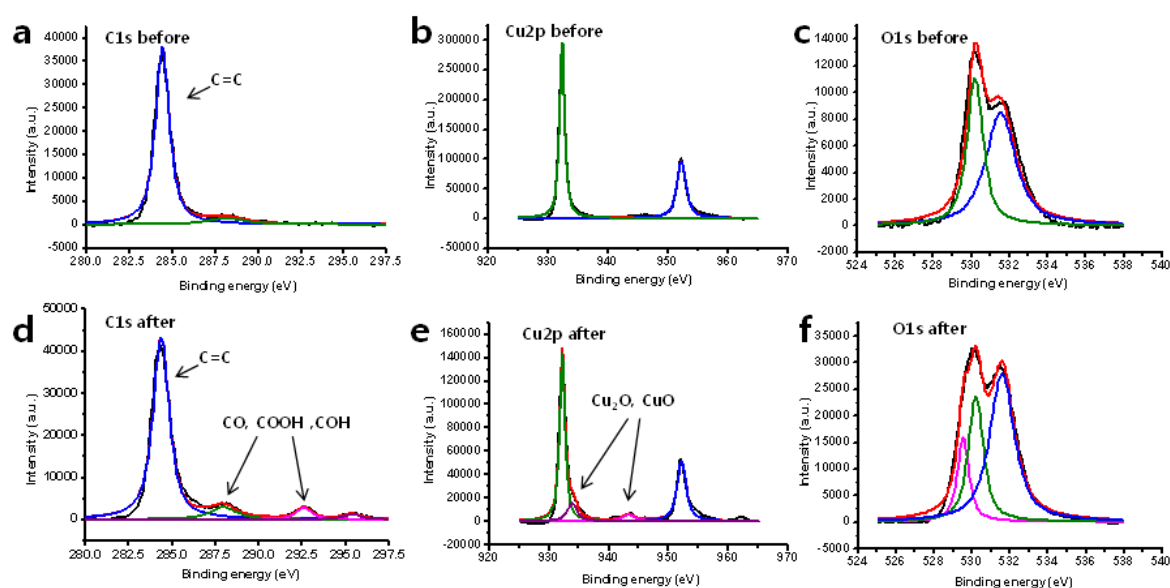


Figure 3S. Raman spectra of Graphene/Cu after 10 days exposure to oxygen in air (black), basic permanganate treatment (red), and acidic permanganate treatment (blue), respectively. (a) D and G bands, (b) the 2D band.

XPS Spectra: XPS shows the functional groups formed on the surface of graphene and copper, which were analyzed by full survey spectra both before and after permanganate treatment Graphene/Cu (Figure 3S). Clean copper shows the presence of the C1s peak (284.3 eV) and Cu2p peak (932.3 eV, 952.16 eV). Deconvolution of the sample after permanganate treatment shows the presence of oxidation of both copper and carbon (peaks of carbon C1s 287.9 eV, 292.6 eV, 295.5 eV and copper Cu2p 933.9 eV, 943.7 eV). However, the intensities of additional peaks were very low compared with graphene oxide³ or copper oxide⁴, which implies that only a partial area⁴ was oxidized. The surface atomic percent ratios of C, O, and Cu were calculated from the corresponding peak areas of the XPS spectra and are summarized as a table in Figure 3S. The ratio of oxygen is significantly increased from 12.87% to 30.17%.



Atomic %	Before treatment	After treatment
Cu2p3	33.03	13.90
C1s	54.10	55.93
O1s	12.87	30.17

Figure 4S. XPS spectra of C1s, O1s, Cu2p peaks before and after permanganate treatment.

Calculation

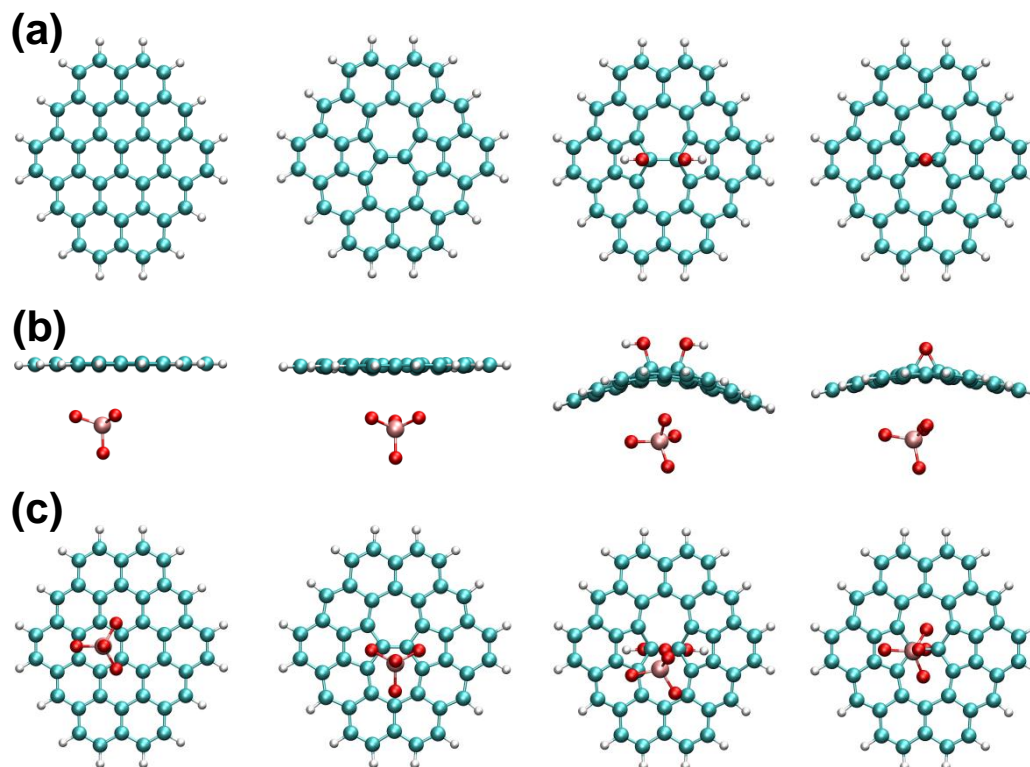


Figure 5S. (a) Top views of the employed graphitic systems representing a clean flake, Stone-Wales defect (SW), SW-glycol, SW-epoxide, from left to right. (b) Side views of graphitic systems below which a permanganate ion is attached. Note that graphitic systems are not deformed noticeably when attached to other chemical species. (c) Bottom views of the graphitic systems when a permanganate ion is adsorbed.

1. Huang, P. Y.; Ruiz-Vargas, C. S.; van der Zande, A. M.; Whitney, W. S.; Levendorf, M. P.; Kevek, J. W.; Garg, S.; Alden, J. S.; Hustedt, C. J.; Zhu, Y.; Park, J.; McEuen, P. L.; Muller, D. A. *Nature* **2011**, 469, (7330), 389-392.
2. Jin, Z.; McNicholas, T. P.; Shih, C.-J.; Wang, Q. H.; Paulus, G. L. C.; Hilmer, A. J.; Shimizu, S.; Strano, M. S. *Chem. Mater.* **2011**, 23, (14), 3362-3370.
3. Chandra, V.; Yu, S. U.; Kim, S. H.; Yoon, Y. S.; Kim, D. Y.; Kwon, A. H.; Meyyappan, M.; Kim, K. S. *Chem. Commun.* **2012**, 48, (5), 735-737.
4. Chen, S.; Brown, L.; Levendorf, M.; Cai, W.; Ju, S.-Y.; Edgeworth, J.; Li, X.; Magnuson, C. W.; Velamakanni, A.; Piner, R. D.; Kang, J.; Park, J.; Ruoff, R. S. *ACS Nano* **2011**, 5, (2), 1321-1327.